Chemistry–A European Journal
Research Article
doi.org/10.1002/chem.202203541
Chemistry Europe
European Chemical Societies Publishing
www.chemeurj.org

Diquat Based Dyes: A New Class of Photoredox Catalysts and Their Use in Aerobic Thiocyanation

Armin Meier,[a] Sabuhi V. Badalov,[b] Timur Biktagirov,[b] Wolf Gero Schmidt,[b] and René Wilhelm*[a]

Abstract: A series of new organic donor–π–acceptor dyes incorporating a diquat moiety as a novel electron-acceptor unit have been synthesized and characterized. The analytical data were supported by DFT calculations. These dyes were explored in the aerobic thiocyanation of indoles and pyrroles. Here they showed a high photocatalytic activity under visible light, giving isolated yields of up to 97%. In addition, the photocatalytic activity of standalone diquat and methyl viologen through formation of an electron donor acceptor complex is presented.

Introduction

The research field of photoredox catalysis has attracted significant scientific interest over the last few decades.[1] Photocatalysts have been employed in applications such as the hydrogen evolution reaction[2] and the removal of organic pollutants from water.[3] However, they are also increasingly recognized as useful tools for organic synthesis and allow for the targeted functionalization of molecules.[4]

Homogeneous photocatalysis requires either organic molecules or metal complexes.[4c,d,5] While noble-metal complexes often provide good photocatalytic activity in a broad variety of reactions,[4c,5a–c] the environmental and toxicity concerns associated with these metals are a disadvantage when considering industrial use, and the limited availability of Ru and Ir is an additional concern.[5d] Hence, the search for new, noble-metal-free alternatives led to the development of complexes based on cheaper transition metals like copper.[6] Furthermore, a number of well-established organic photocatalysts have been reported.[4d,5b,e–s]

Yet, interestingly the large common family of linear organic push–pull dyes with a D-π-A structure found in Grätzel cells[7] have been less frequently applied as photocatalysts.[8] This is certainly due to the fact that the HOMO–LUMO levels in most of these dyes are not beneficial for organic redox reactions. Furthermore, these dyes often have a short lifetime of their excited state. Although this is suitable in the application as photosensitizers, for example, with TiO_2,[7] it is disadvantageous for homogenous photoredox catalytic organic transformations. A common blueprint for these organic dyes consists of a conjugated π-system connecting an electron-rich donor moiety to an electron-poor acceptor moiety. Such donor–π-bridge-acceptor dyes (D-π-A dyes) can then be tuned in their properties by modifying the individual structural elements.[9] Minor changes can already have a large impact on their properties.[7a,10]

Diquat, the ethylene-bridged dicationic derivate of 2,2′-biypridine, is an interesting moiety for the use in D-π-A dyes.[11] The ring system can undergo reversible one- and two-electron reductions to form a radical cation and a neutral species.[12] The redox-cycling ability promotes the generation of superoxide radicals and related reactive species. This is thought to be the main contributor to the cytotoxic activity of diquat dibromide, which is used as a herbicide.[13] In addition, due to the formation of stable radicals, diquat and its 4,4′-bipyridine analogue have been used as radical mediators in several applications.[14] Recently it was also shown that the photocatalytic hydrogen evolution activity of a covalent organic framework could be increased by introducing diquat moieties into the structure through an improved electron transfer.[15] As an alkyl-pyridinium derivate, the electron-poor rings of the diquat moiety are a natural acceptor unit in a D-π-A dye. Indeed, dyes with a quaternized pyridinium acceptor, among others, have been used as photoactivated antimicrobial compounds[16] and photosensitizers for the titania-catalyzed hydrogen evolution reaction of water.[7d] On the other hand, photocatalytic active D-π-A dyes with a diquat moiety as the acceptor have, to the best of our knowledge, not yet been reported so far as organic photocatalysts.

In this study, we present a number of novel diquat-based D-π-A dyes. The UV-vis spectra and cyclic voltammograms of these new compounds were measured and compared to values predicted by DFT calculations. The photocatalytic activity of the

[a] A. Meier, Prof. Dr. R. Wilhelm
Institute of Organic Chemistry
Clausthal University of Technology
Leibnizstr. 6, 38678 Clausthal-Zellerfeld (Germany)
E-mail: rene.wilhelm@tu-clausthal.de

[b] S. V. Badalov, Dr. T. Biktagirov, Prof. Dr. W. G. Schmidt
Lehrtuhl für Theoretische Materialphysik
Universität Paderborn
33095 Paderborn (Germany)

Supporting information for this article is available on the WWW under https://doi.org/10.1002/chem.202203541

dyes was explored in the aerobic thiocyanation of indole and related molecules with very high yields.

Results and Discussion

Thiophene offers desirable properties for the use as a π-bridge in D-π-A dyes. Its aromaticity makes it less susceptible to attack and chemical decomposition than olefinic double bonds, while its geometry allows for smaller twist angles between neighboring aromatic rings compared to phenyl–phenyl bonds.[17] Its relatively higher electron density allows it to also act as a weak electron donor, rather than just an extension of the conjugated system. The 2-position in thiophenes is sufficiently reactive to allow for palladium-catalyzed cross-couplings with aryl bromides without the need for additional functionalization. Hence, a synthesis protocol from Fujinami et al.[18] were adapted for the synthesis of the desired new dyes.

The general synthetic pathway for the donor moieties is depicted in (Scheme 1A). For the synthesis of **5** in this fashion, the fact that both substrates contain two attackable positions means that undesired oligomerizations can occur, reducing the yield. However, conducting the reaction in a closed pressure flask with a large excess of thiophene suppressed the oligomerization and provided yields of over 50%. Similarly, coupling reactions of a building block with two terminal thiophene rings, such as **5** and **8**, do allow for the formation of dicoupled product, but using said building block in excess provided yields greater than 50%, while most of the unreacted excess substrate could be recovered following workup and column chromatography.

For connecting the bipyridine and donor moieties, first coupling reactions using **5** and 4-bromo-2,2′-bipyridine **9** were explored. However, no desired product was isolated (Scheme 1B). It was assumed that the 2,2′-bipyridine moiety, as a natural bidentate ligand, binds strongly on the palladium catalyst and inhibits the intended coupling reaction. Hence, the corresponding *N*-oxide **10** of 4-bromobipyridine was applied, which gave products **1a**–**3a** in yields of 59, 67 and 51%, respectively.

After the final coupling, the reduction of the *N*-oxides **1a**–**3a** with zinc and ammonium chloride gave the bipyridines **1b**–**3b** in up to 87% yield, which were transformed into the diquat dibromide forms **1c**–**3c** under reflux in neat 1,2-dibromoethane. An ion exchange with $NaPF_6$ yielded the final products in up to 66% yield over two steps. Overall, three new diquat dyes were synthesized in this fashion: TPTDQPF$_6$ **1d**, TTDQPF$_6$ **2d**, and TPATPTDQPF$_6$ **3d** (Scheme 2).

The dicationic character of the diquat moiety combined with the extended tail of the aromatic rings resulted in a low solubility of the new DQ dyes in several solvents, being insoluble in water as well as in organic solvents of medium or low polarity. The bromide salts were lightly soluble in alcohols, while exchanging the counterion to hexafluorophosphate improves the solubility in polar aprotic solvents such as acetonitrile, THF and DMF, as expected. Especially these solvents are predominately applied in photoredox reactions.[4c,5a–c] Upon dissolving in acetonitrile, TPATPTDQPF$_6$ **3d** formed a wine-red solution while the other dyes gave orange-red solutions. The UV-vis spectra (Figure 1) show broad absorptions with the first maxima in the cyan area for TPTDQPF$_6$

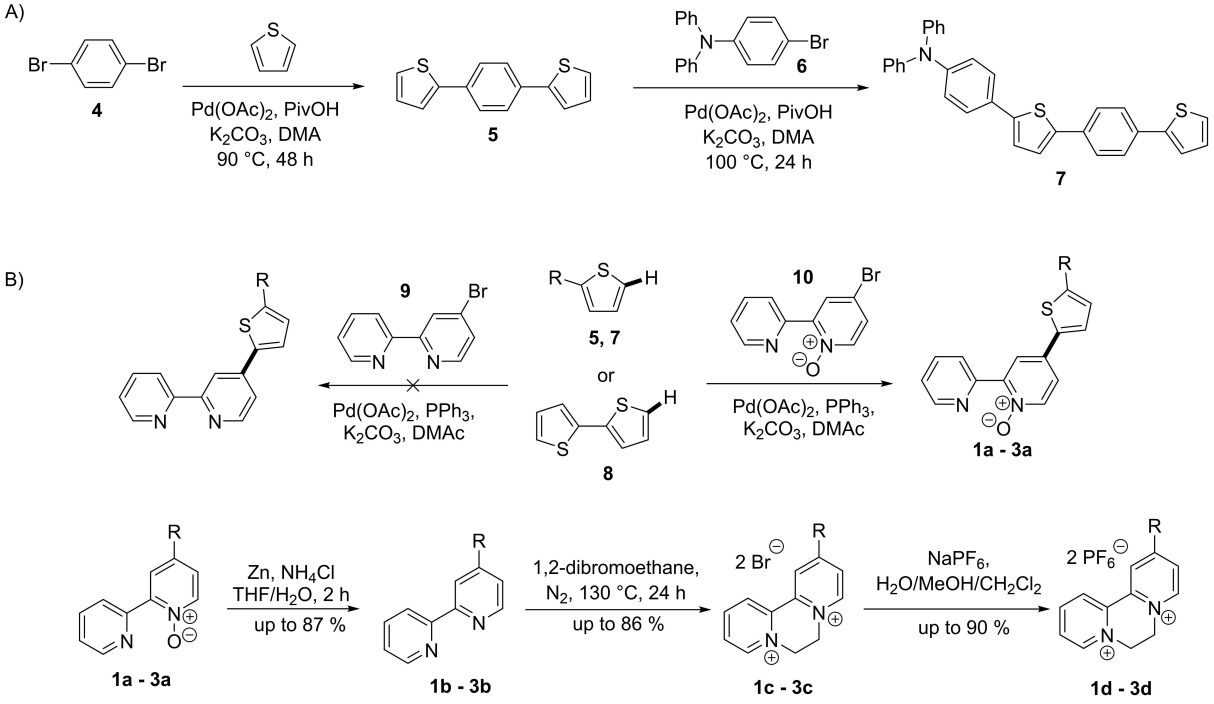

Scheme 1. Synthesis pathway of the new dyes: A) the donor moieties, B) the dyes.

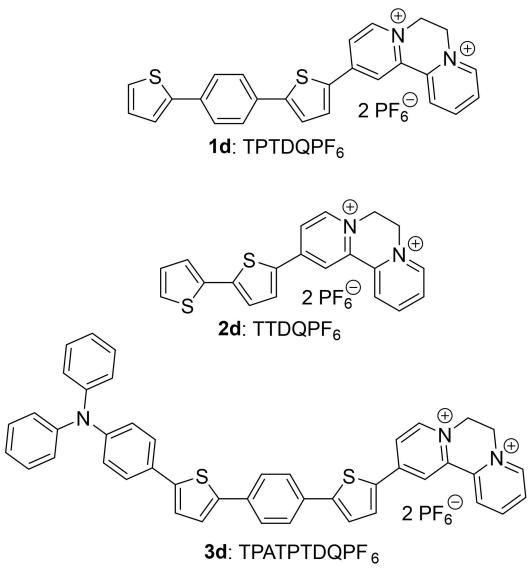

Scheme 2. Structure of the diquat dyes.

1 d (473 nm) and $TTDQPF_6$ **2 d** (467 nm), and in the green area for $TPATPTDQPF_6$ **3 d** (507 nm).

The redox potentials were investigated using cyclic voltammetric measurements (Figure 1). The reduction of the DQ dyes **1 d**–**3 d** showed a reversible two-step reduction in line with the expected formation of a radical cation and a neutral species, respectively. With potentials of approximately −0.16 and −0.55 V for the first and second reduction, the substrate scope for catalytic reductions of organic molecules would be limited,[19] but an oxidative quenching by O_2 is possible. The oxidation potential for **1 d** was measured to be approximately +1.6 V, which is sufficient to enable oxidations of electron-rich organic molecules. The oxidation potential for **2 d** was not observed in the CV under the chosen conditions, but should be expected to be greater than that of **1 d**. Due to the strong electron-donating abilities of the triphenylamine, **3 d** possesses a much lower oxidation potential of approximately +1.09 V, and a second oxidation occurs at +1.26 V.

These experimental results were complemented by DFT[20] and TDDFT[21] calculations. The DFT-calculated HOMO and LUMO energy levels are shown in Figure 2a, and the electron density distribution over the frontier molecular orbitals

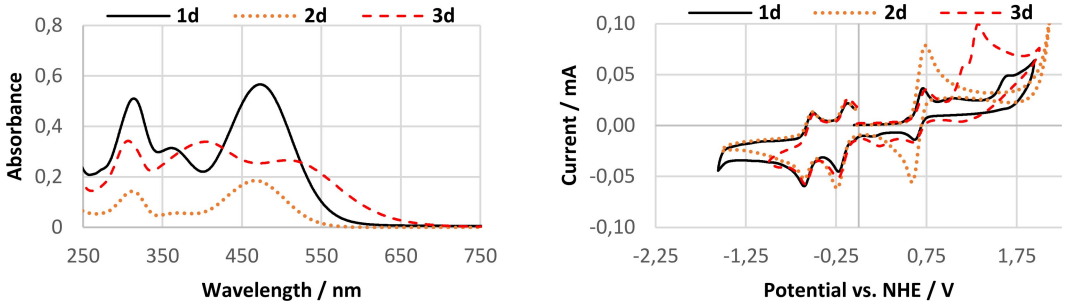

Figure 1. Left: UV-vis spectra of the dyes **1 d**–**3 d**, measured in MeCN; Right: cyclovoltammograms of the dyes, measured in DMF with ferrocene as internal standard.

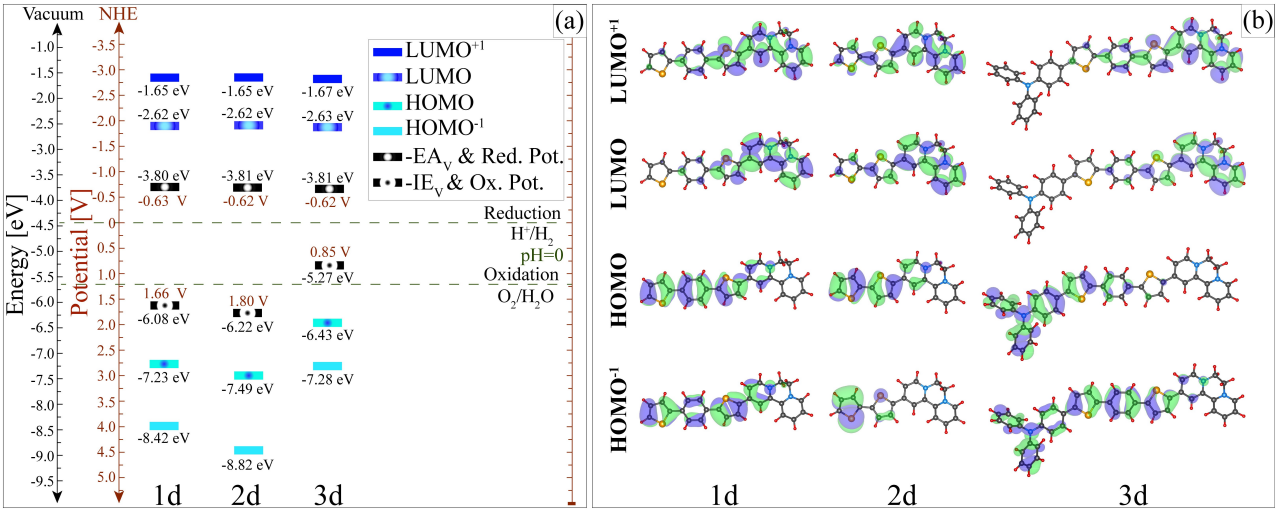

Figure 2. a) Calculated energies of the frontier molecular orbitals (HOMO−1, HOMO, LUMO, LUMO+1), and redox and oxidation potential of dyes **1 d**, **2 d**, and **3 d** in relation to the redox reactions of water splitting. b) Isosurface plots of the HOMO−1, HOMO, LUMO, and LUMO+1 orbitals of **1 d**, **2 d**, and **3 d**.

(HOMO−1, HOMO, LUMO, and LUMO+1) is illustrated in Figure 2b.

For all three dyes with the diquat electron-acceptor moiety, **1d**, **2d**, and **3d**, the electron density distribution over the frontier orbitals is indicative of the intramolecular charge transfer (ICT). The electron density of the LUMO of these three dyes clearly shows predominant localization on the diquat moiety. Their HOMO electron density is localized on the electron-donating parts showing the overlap with the LUMO at the π-linker. These results confirm that the HOMO–LUMO transition in **1d**, **2d** and **3d** is accompanied by the intramolecular charge transfer from the electron-donor unit to the acceptor moiety through the π-linker. The more pronounced separation of the HOMO and LUMO electron densities in **1d** and **3d** is expected to result in the prolonged lifetime of photoexcited carriers compared to **2d**.[22] Since **1d**, **2d**, and **3d** share the same acceptor moiety, they expectedly manifest almost the same LUMO energy around −2.6 eV. As for the HOMO energy, it depends on the electron-donating abilities of the donor part. For example, the strongly electron-donating triphenylamine group used in **3d** leads to the significantly higher HOMO energy (−6.43 eV) compared to **1d** and **2d**. Accordingly, the calculated HOMO–LUMO energy gaps of these three dyes thus increase in the following order **3d**<**1d**<**2d** with the corresponding values of 4.61 eV for **1d**, 4.87 eV for **2d**, and 3.80 eV for **3d**. Details for calculated reduction and oxidation potentials are given on p. S6 in the Supporting Information.

The absorption spectra of the dyes **1d**, **2d** and **3d** computed using TDDFT are shown in Figure 3. Remarkably, the positions of the first maxima of the **1d** (457 nm), **2d** (450 nm) and **3d** (536 nm) dyes are in very good agreement with the experimental data. In all cases, the absorption spectra exhibit the most intense peak in the visible light range that we find to be dominated by the single-electron HOMO–LUMO transition, as expected for D-π-A dyes.[23] The calculated lifetime of the exited states for the catalysts was around 1.5 ns, which is sufficient for photocatalytic applications (for details see p. S7 in the Supporting Information) yet smaller compared to some common photocatalysts[24] but larger than other dyes which have lifetimes in the ps range.[25]

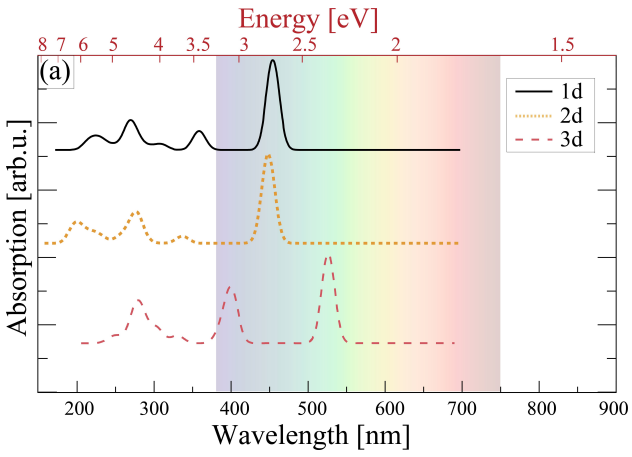

Figure 3. Absorption spectra of the diquat dyes as calculated with TDDFT. The spectra were simulated by using 20 nm Gaussian broadening.

The photostability of the dyes was analyzed by irradiating a 0.01 M solution of the dye in MeCN with an appropriate wavelength LED (460 nm for **1d** and **2d**, 515 nm for **3d**) for 16 h under air. Samples of the solutions before and after the irradiation were taken, diluted by a factor of 50, and the UV spectra compared. No significant change in the spectra was observed, indicating sufficient photostability of the catalysts.

Next, the catalytic activity of the new dyes was evaluated in an aerobic thiocyanation of indoles and related heterocycles. The latter reaction is a useful C–S bond formation and has been conducted under a variety of conditions. Originally performed using toxic and reactive cyanogen,[26] methods using thiocyanate salts such as NH_4SCN were developed. These require either stoichiometric amounts of further reactants, such as *N*-chlorosuccinimide[27] and hypervalent iodine compounds,[28] or a suitable catalyst to use elemental oxygen as the oxidant.[29] This has been achieved by photocatalysis with heterogeneous inorganic catalysts[30] and by organic photocatalysts.[30–31] In these reactions, the oxidation of the SCN ion appears to be the initiating step. As the oxidation potential of the SCN-anion is between +0.8 and +0.9 V versus NHE,[32] the calculations and CV measurements indicated that $TPTDQPF_6$ **1d** and $TTDQPF_6$ **2d** should be suitable for this reaction, while **3d** may or may not be. The optimization of the reaction conditions, as well as control and benchmark reactions, are presented in Table 1.

The reaction was first explored by using **1d** as the catalyst and MeCN as the solvent (see p. S4 in the Supporting Information for solubility data of **1d**). When using a 460 nm LED as a light source, it led to a significant increase in yield (Table 1, run 6) compared to the catalyst-free reaction (Table 1, run 5), but the overall reaction rate was low. Changing the solvent to dioxane provided an improved yield compared to MeCN (Table 1, run 11). Conducting the reaction in THF provided a decent yield of 73% after 8 h (Table 1, run 8). The performance under white LED-light was not favorable (Table 1, run 9), likely because the emission spectrum of the used white LEDs had a minimum between 460 and 520 nm (see p. S2 in the Supporting Information), which is the same region as the dye's absorption maximum. Extending the reaction time to 16 h provided full conversion with a yield of 92% (Table 1, run 1). Even with a reduced catalyst loading of 0.1 mol%, a decent yield of 57% was achieved within 8 h (Table 1, run 10). During control reactions, no catalytic effect with **1d** was observed when the reaction was carried out under a nitrogen atmosphere (Table 1, run 13), and no reaction was observed in the absence of light even after 24 h (Table 1, run 12).

After the optimization of conditions with **1d**, the other two dyes were investigated in the reaction. Compound **3d** did not appear to catalyze the reaction at all when irradiated with the appropriate light for 8 h (Table 1, run 18). As anticipated from the CV measurements, the energy of the LUMO is likely not high enough to reliably oxidize the thiocyanate under the reaction conditions. The catalytic performance of **2d** was in the range of **1d**, providing slightly lower yields of 66% in THF but

Table 1. Optimization of conditions for the thiocyanation of indole.

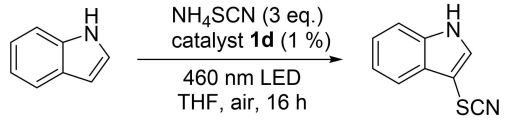

No	Catalyst	Deviation from optimized conditions	Yield[a] [%]
1	**1 d**	–	92
2	–	white LED, 8 h, no catalyst	10
3	–	490 nm LED, in MeCN, 8 h, no catalyst	3
4	**1 d**	490 nm LED, in MeCN 8 h	9
5	–	in MeCN, 8 h	7
6	**1 d**	in MeCN, 8 h	29
7	–	8 h, no catalyst	15
8	**1 d**	8 h	73
9	**1 d**	white LED, 8 h	43
10	**1 d**	0.1 % catalyst loading	57
11	**1 d**	in dioxane, 8 h	47
12	**1 d**	in darkness, 24 h	n.d.
13	**1 d**	under nitrogen atmosphere	10
14	RB[b]	white LED, 8 h	91
15	Mes-Acr$^+$[c]	8 h	71
16	**2 d**	8 h	66
17	**2 d**	in MeCN, 8 h	43
18	**3 d**	515 nm LED, 8 h	n.d.
19	**11**	8 h	48
20	**11**	in darkness	n.d.
21	**12**	8 h	42
22	**12**	in darkness	n.d.
23	**11**	50 % catalyst loading, in darkness	n.d.
24	**12**	50 % catalyst loading, in darkness	n.d.
25	**1 d**	addition of 3 equiv. TEMPO	5
26	**1 d**	addition of 3 equiv. 1,1-diphenylethylene	67

[a] Isolated yields. [b] Rose Bengal. [c] Fukuzumi's catalyst.

required for the catalytic activity of the diquat (Table 1, runs 19 and 20). Therefore, we measured the impact of the other reaction components on the diquat's UV-vis spectrum in THF. Upon addition of NH_4SCN, the absorption at 310 nm decreased, while a very broad new absorption band with a maximum at 477 nm appeared (Figure 4). This behavior suggests the in-situ formation of an electron-donor–acceptor (EDA) complex between the cationic aromatic diquat and the thiocyanate anion (Scheme 3). The formation of EDA complexes and that they are excitable by visible light has been known and used as a tool for photocatalytic transformations.[33] This would explain the observed behavior of diquat **11**. As the new absorption band increases further with increasing excess of NH_4SCN but not with time, the formation of the complex appears to be fast and reversible, with the equilibrium on the side of the free ions under the measurement conditions. A similar observation was made for the hexafluorophosphate salt of the diquat-related molecule methyl viologen (paraquat) **12**. Under the same conditions, it provided a slightly lower yield of 42 %, and no yield under absence of light (Table 1, runs 21 and 22). In the UV-vis spectrum, the addition of NH_4SCN caused the emergence of a new peak with a maximum at 398 nm and a very broad peak to reach across the visible spectrum (Figure 4). Interestingly, conducting the spectroscopic investigation with **1 d** and NH_4SCN showed no strong impact of the thiocyanate salt on the innate absorption of the dye (see p. S6 in the Supporting Information). This suggests that unlike **11** and **12**, **1 d** might not

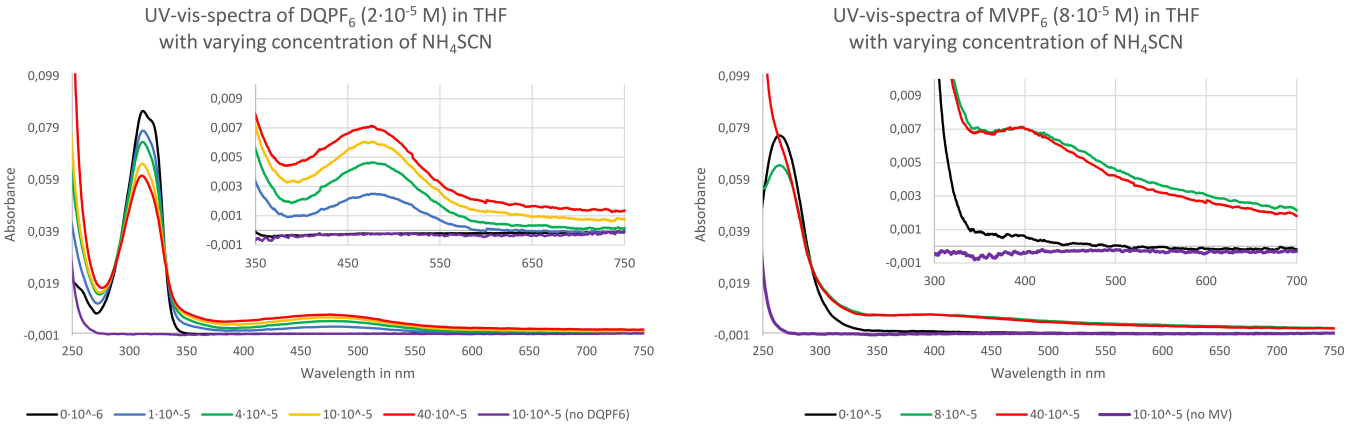

Figure 4. Absorption spectra of diquat PF_6 (**11**, left) and methyl viologen PF_6 (**12**, right) in THF with various concentrations of NH_4SCN, and of NH_4SCN in THF.

higher yields of 43 % in MeCN after 8 h, respectively (Table 1, runs 16 and 17). Benchmark reactions with Rose Bengal (Table 1, run 14, originally reported by Fan et al.[31] and Fukuzumi's catalyst (run 14) showed that **1 d** has a good competitive catalytic activity. To investigate the standalone reactivity of the diquat moiety, we conducted reactions using diquat hexafluorophosphate **11** as the catalyst. Although **11** does not adsorb light in the visible range a moderate yield of 48 % was obtained after 8 h under normal reaction conditions. A control reaction in darkness showed that the blue light was rely on the formation of an EDA complex for its photocatalytic activity. However, solubility tests showed that the presence of NH_4SCN significantly increased the solubility of **1 d** in THF and dioxane (see p. S4 in the Supporting Information). An association of the ions in solution, such as in an EDA complex, is therefore likely. As a final investigation, we conducted the thiocyanation with half-stoichiometric amounts of **11** or **12** in the absence of light, but even at such a high loading, no product was observed (Table 1, runs 23 and 24). This confirms our expectation that light is required for the initiation of the reaction and not just for the regeneration of the catalyst.

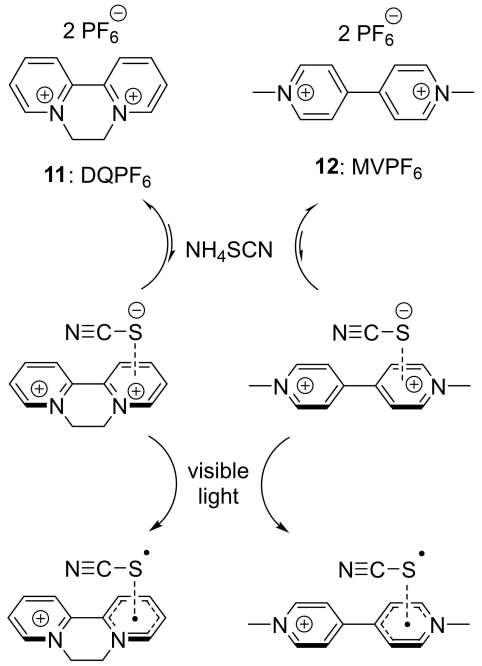

Scheme 3. Formation of electron-donor–acceptor complexes of **11** and **12**.

With the optimized conditions at hand, the catalyst TPTDQPF$_6$ **1 d** was explored in the reaction with other indole analogs to determine the substrate scope of the reaction (Scheme 4). While electron-withdrawing substituents on the indole slowed down the rate of conversion, they do not appear to prevent the formation of the intended products, allowing yields of up to 97% for **18**. 4-Methoxy-indole and 2-methylindole gave lower yields of 83% for **16** and 74% for **17** even after full conversion. It is conceivable that such electron-rich derivatives can undergo undesired side reactions.

The analogous benzothiophene as well as 2,2′-bithiophene appeared unreactive under the presented conditions and no desired **22** and **23** were formed. A reaction with pyrrole gave full conversion after 24 h; however, the desired product **24** was isolated in only 24% yield. Most of the substrate appears to have oligomerized or otherwise oxidized to different species during the reaction. The product that was isolated after chromatography was identified as 2-thiocyanato-pyrrole (**24**) by NMR spectroscopy, albeit with impurities due to the sensitivity of the compound. This product is expected as the 2-position in pyrroles is generally more reactive than the 3-position. Hence, we also explored the reactivity of 2,5-disubstituted pyrrole derivatives in the reaction. The reactions proceeded successfully, resulting in monosubstitution at the 3-position of the molecules, yielding the new compounds **26**–**28** that to our knowledge are unreported in the literature thus far. The reactions proceeded faster and provided higher yields compared to **24**, but in a moderate range. In the case of the unsymmetric **27**, a 1:0.9 mixture of the two possible regioisomers was obtained. It appears the electronic and steric differences of the substituents did not have a significant impact on a possible regioselective formation of **27 a** or **27 b**.

To gain further insight into the mechanism of the reaction, test reactions in the presence of a threefold excess of TEMPO-radical or 1,1-diphenylethylene (Table 1, runs 25 and 26) were conducted. The addition of TEMPO strongly inhibited the reaction, providing only 5% yield after 16 h, with the majority of substrate being recovered. Diphenylethylene also reduced the amount of product obtained to 67%, comparable to the

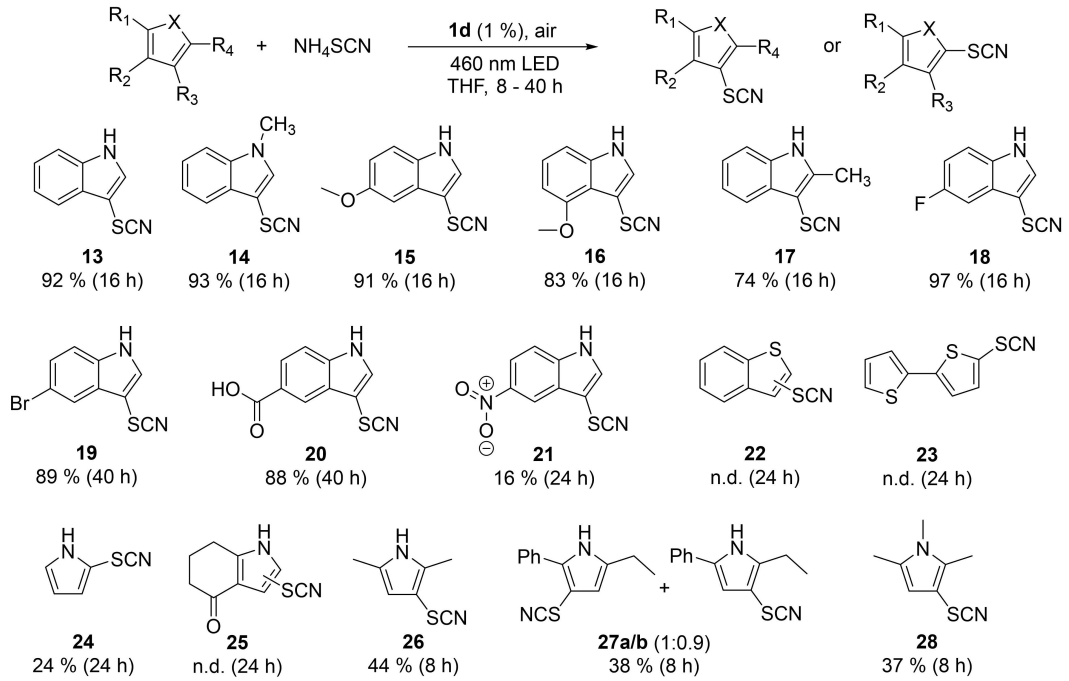

Scheme 4. Product scope of the thiocyanation reaction with **1 d** with isolated yields after purification by chromatography.

amount normally obtained in half that time. At the same time, addition products of diphenylethylene and thiocyanate were observed in the product mixture. The main product was 2-thiocyanato-1,1-diphenylethanol **29**, obtained in 18% yield (55% relative to the used amount of indol), but traces of 1,1-diphenyl-2-thiocyanatoethylene **30** were also observed. The fact that TEMPO completely quenched the reaction while diphenylethylene merely competed with the desired reaction suggests that the mechanism of inhibition might differ. While it is possible that TEMPO is just a more reactive radical interceptor, another explanation is that TEMPO can reductively quench the excited catalyst. The oxidation potential of TEMPO has been reported to be 0.2–0.3 V vs. $Ag/AgNO_3$ (0.4–0.5 V vs. NHE),[34] which is significantly lower than that of NH_4SCN. It is therefore likely that TEMPO acts as a reductive quencher, rather than a radical interceptor.

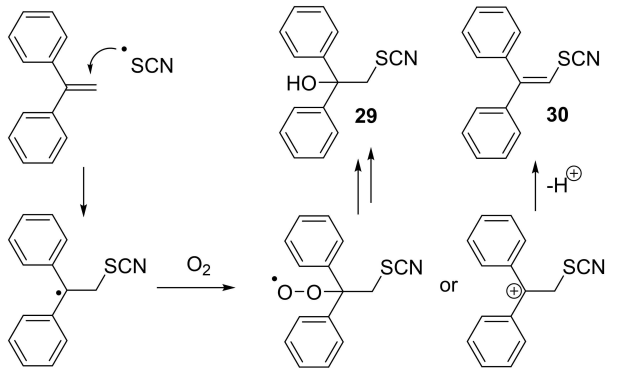

Scheme 5. Formation of the observed products **29** and **30** after interception of the thiocyanate radical by 1,1-diphenylethylene.

According to literature similar reactions were reported where the function of the photocatalyst was the oxidation of thiocyanate to its radical.[31] This fits with our own observation of addition products, which could result through the addition of the SCN radical to the olefinic double bond, followed by either addition of oxygen or by oxidation through oxygen and subsequent deprotonation, respectively (Scheme 5). In fact, that precise reaction has been described by Zhang et al. for the targeted synthesis of β-thiocyanatoalcohols.[35]

Comparing our own observations and computational results with the literature, we therefore propose a mechanism for the diquat-based dyes as depicted in Scheme 6 with **1 d** as the example. The dye is excited by visible light, causing a charge transfer from the donor moiety to the diquat moiety. The now electron deficient donor oxidizes the thiocyanate into the respective radical while reducing the catalyst into its radical-cation species. The catalyst is then oxidized to its original state by atmospheric oxygen. The thiocyanyl radical attacks the heterocycle at the electron-rich double bond, forming the most stable intermediate. This is an attack in the 2-position for pyrroles and in the 3-position for indoles and 2,5-disubstituted pyrroles. The resulting addition intermediate is quickly oxidized by the ambient oxygen, leading to a cationic intermediate. Re-aromatization by the abstraction of a proton forms the product. For **11** and **12** a similar mechanism can be expected, however, since the adsorption of visible light of the pure EDA complexes is significantly lower, the catalytic activity is also lower compared to **1 d**.

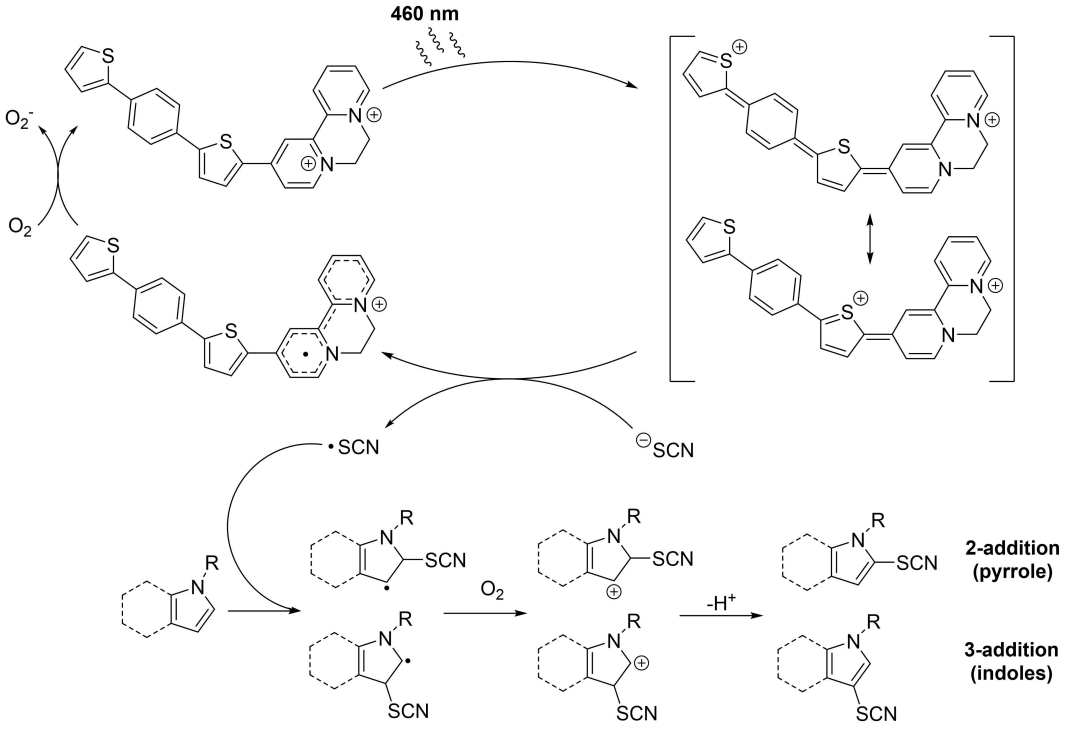

Scheme 6. Proposed mechanism for the thiocyanation of indoles and pyrroles with **1 d** as the catalyst.

Conclusion

In conclusion, we have synthesized a new class of D-π-A dyes as photocatalysts with a diquat moiety as their acceptor group. Theoretical calculations using density functional theory provided the electronic characteristics of these dyes and confirmed their intramolecular charge transfer behavior. The high photocatalytic activity of two of these dyes has been demonstrated in the aerobic thiocyanation of indole and pyrrole derivates. The substrate scope of the reaction was explored with up to 97% isolated yields, and the synthesis of new thiocyanatopyrroles is reported. We also observed the photocatalytic activity of diquat and methyl viologen, which likely involves the formation of EDA complexes with the thiocyanate anion. The connection of electron-donor systems significantly improved the visible-light absorption and catalytic activity compared to the stand-alone diquat ion. As the individual moieties of the D-π-A dyes can be easily modified to tailor their properties, our findings open up a broad new category of potential photocatalysts. In addition, the observed catalytic activity of the EDA complexes with **11** and **12** will result in new photocatalytic applications of diquat **11** and viologen **12**.

Experimental Section

General procedure for the catalytic thiocyanation of various substrates using 1 d as catalyst: To a small round bottom flask with stirring bar were added 0.50 mmol of substrate, NH_4SCN (114 mg, 1.5 mmol, 3 equiv.), 1d $TPTDQPF_6$ (3.6 mg, 0.005 mmol, 1%), and 5 mL of THF. The mixture was stirred in the open flask and irradiated from below by a 3 W LED with an emission maximum of 460 nm and without significant emission below 410 nm. Heating of the setup was prevented through a water-cooled metal cooling block. The reaction setup was covered from outside light and the reaction progress monitored with TLC. After 8/16/24/40 h, the reaction mixture was diluted with CH_2Cl_2 and filtered. The solvent was evaporated and the residue separated through column chromatography using a mixture of petrol ether/ethyl acetate.

Acknowledgements

We gratefully acknowledge funding from the Deutsche Forschungsgemeinschaft (DFG) under projects no. SCHM 1361/25, SCHM 1361/26, and WI 2147/17. Open Access funding enabled and organized by Projekt DEAL.

Conflict of Interest

The authors declare no conflict of interest.

Data Availability Statement

The data that support the findings of this study are available in the Supporting Information material of this article. Supporting Information Accepted Article.pdf.

Keywords: donor–acceptor dye systems · diquat · photocatalysis · thiocyanation

[1] a) B. König, *Chemical Photocatalysis*, De Gruyter, Berlin, **2013**; b) S. G. Amos, M. Garreau, L. Buzzetti, J. Waser, *Beilstein J. Org. Chem.* **2020**, *16*, 1163–1187.
[2] W. Zhao, Z. Chen, X. Yang, X. Qian, C. Liu, D. Zhou, T. Sun, M. Zhang, G. Wei, P. D. Dissanayake, Y. Ok, *Renewable Sustainable Energy Rev.* **2020**, *132*, 110040.
[3] V.-H. Nguyen, S. M. Smith, K. Wantala, P. Kajitvichyanukul, *Arab. J. Chem.* **2020**, *13*, 8309–8337.
[4] a) X. Zhang, K. P. Rakesh, L. Ravindar, H.-L. Qin, *Green Chem.* **2018**, *20*, 4790; b) R. Cannalire, S. Pelliccia, L. Sancineto, E. Novellino, G. T. Tron, M. Giustiniano, *Chem. Soc. Rev.* **2021**, *50*, 766–897; c) J. J. Douglas, M. J. Sevrin, C. R. Stephenson, *Org. Process Res. Dev.* **2016**, *20*, 1134–1147; d) N. A. Romero, D. A. Nicewicz, *Chem. Rev.* **2016**, *116*, 10075–10166; e) J.-P. Goddard, C. Ollivier, L. Fensterbank, *Acc. Chem. Res.* **2016**, *49*, 1924–1936; f) R. A. Angnes, Z. Li, C. R. D. Correia, G. B. Hammond, *Org. Biomol. Chem.* **2015**, *13*, 9152–9167; g) L. Buzzetti, G. E. M. Crisenza, P. Melchiorre, *Angew. Chem. Int. Ed.* **2019**, *58*, 3730–3747; *Angew. Chem.* **2019**, *131*, 3768–3786; h) M. H. Shaw, J. Twilton, D. W. C. MacMillan, *J. Org. Chem.* **2016**, *81*, 6898–6926; i) I. Ghosh, L. Marzo, A. Das, R. Shaikh, B. König, *Acc. Chem. Res.* **2016**, *49*, 1566–1577; j) L. Marzo, S. K. Pagire, O. Reiser, B. König, *Angew. Chem. Int. Ed.* **2018**, *57*, 10034–10072; *Angew. Chem.* **2018**, *130*, 10188–10228.
[5] a) K. Teegardin, J. I. Day, J. Chan, J. Weaver, *Org. Process Res. Dev.* **2016**, *20*, 1156–1163; b) J. D. Bell, J. A. Murphy, *Chem. Soc. Rev.* **2021**, *50*, 9540–9685; c) X.-Y. Yu, J.-R. Chen, W.-J. Xiao, *Chem. Rev.* **2021**, *121*, 506–561; d) I. K. Sideri, E. Voutyritsa, C. G. Kokotos, *Org. Biomol. Chem.* **2018**, *16*, 4596; e) K. Murugesan, K. Donabauer, R. Narobe, V. Derdau, A. Bauer, B. König, *ACS Catal.* **2022**, *12*, 3974–3984; f) S. A. Deshmukh, P. R. Bhagat, *ChemistrySelect* **2022**, *7*, e202200189; g) H. Li, O. S. Wenger, *Angew. Chem. Int. Ed.* **2022**, *61*, e202110491; h) W. H. García-Santos, J. Ordóñez-Hernández, M. Farfán-Paredes, H. M. Castro-Cruz, N. A. Macías-Ruvalcaba, N. Farfán, A. Cordero-Vargas, *J. Org. Chem.* **2021**, *86*, 16315–16326; i) A. Tlili, S. Lakhdar, *Angew. Chem. Int. Ed.* **2021**, *60*, 19526–19549; *Angew. Chem.* **2021**, *133*, 19678–19701; j) C. Bottecchia, R. Martín, I. Abdiaj, E. Crovini, J. Alcazar, J. Orduna, M. J. Blesa, J. R. Carrillo, P. Prieto, T. Noel, *Adv. Synth. Catal.* **2019**, *361*, 945–950; k) N. F. Nikitas, P. L. Gkizis, C. G. Kokotos, *Org. Biomol. Chem.* **2021**, *19*, 5237–5253; l) M. Vellakkaran, S. Hong, *Asian J. Org. Chem.* **2021**, *10*, 1012–1023; m) C. Rosso, G. Filippini, M. Prato, *Eur. J. Org. Chem.* **2021**, 1193–1200; n) L. Mei, T. Gianetti, *Synlett* **2021**, *32*, 337–343; o) K. Murugesan, K. Donabauer, B. König, *Angew. Chem. Int. Ed.* **2021**, *60*, 2439–2445; *Angew. Chem.* **2021**, *133*, 2469–2475; p) A. Vega-PeÇaloza, J. Mateos, X. Companyl, M. Escudero-Casao, L. Dell'Amico, *Angew. Chem. Int. Ed.* **2021**, *60*, 1082–1097; *Angew. Chem.* **2021**, *133*, 1096–1111; q) Y. Lee, M. S. Kwon, *Eur. J. Org. Chem.* **2020**, 6028–6043; r) J. Cervantes-González, D. A. Vosburg, S. E. Mora-Rodriguez, M. A. Vázquez, L. G. Zepeda, C. V. Gómez, S. Lagunas-Rivera, *ChemCatChem* **2020**, *12*, 3811–3827; s) E. Speckmeier, T. G. Fischer, K. Zeitler, *J. Am. Chem. Soc.* **2018**, *140*, 15353–15365; t) S. Fukuzumi, K. Ohkubo, *Org. Biomol. Chem.* **2014**, *12*, 6059–6071.
[6] a) J.-M. Kern, J.-P. Sauvage, *J. Chem. Soc. Chem. Commun.* **1987**, 546–548; b) C. Minozzi, A. Caron, J.-C. Grenier-Petel, J. Santandrea, S. K. Collins, *Angew. Chem. Int. Ed.* **2018**, *57*, 5477–5481; *Angew. Chem.* **2018**, *130*, 5575–5579; c) D. B. Bagal, G. Kachkovskyi, M. Knorn, T. Rawner, B. M. Bhanage, O. Reiser, *Angew. Chem. Int. Ed.* **2015**, *54*, 6999–7002; *Angew. Chem.* **2015**, *127*, 7105–7108; d) X. Zhu, X. Song, X. Li, F. Wang, J. Lv, M. Jiang, D. Yang, *Adv. Synth. Catal.* **2022**, *364*, 4384–4391.
[7] a) A. Mishra, M. K. R. Fischer, P. Bäuerle, *Angew. Chem. Int. Ed.* **2009**, *48*, 2474–2499; *Angew. Chem.* **2009**, *121*, 2510–2536; b) S. Chaurasia, J. T. Lin, *Chem. Rec.* **2016**, *16*, 1311–1336; c) S. Ahmad, E. Guillen, L. Kavan, M. Grätzel, M. K. Nazeeruddin, *Energy Environ. Sci.* **2013**, *6*, 3439–3466; d) D. D. Konieczna, H. Biller, M. Witte, W. G. Schmidt, A. Neuba, R.

Wilhelm, *Tetrahedron* **2018**, *74*, 142–149; e) L. Kloo, *Chem. Commun.* **2013**, *49*, 6580–6583; f) J. Willkomm, K. L. Orchard, A. Reynal, E. Pastor, J. R. Durrant, E. Reiser, *Chem. Soc. Rev.* **2016**, *45*, 9–23; g) Y. Ma, X. Wang, Y. Jia, X. Chen, H. Han, C. Li, *Chem. Rev.* **2014**, *114*, 9987–10043; h) Y. Wu, W. Zhu, *Chem. Soc. Rev.* **2013**, *42*, 2039–2058.
[8] a) L. Wang, J. Byun, R. Li, W. Huang, K. A. I. Zhanga, *Adv. Synth. Catal.* **2018**, *360*, 4312–4318; b) Z. Wang, H. Li, Z. Wang, M. Suleman, Y. Wang, P. Lu, *J. Org. Chem.* **2021**, *86*, 8101–8111; c) A. R. O. Kosso, N. Sellet, A. Baralle, M. Cormier, J.-P. Goddard, *Chem. Sci.* **2021**, *12*, 6964–6968.
[9] B.-G. Kim, K. Chung, J. Kim, *Chem. Eur. J.* **2013**, *19*, 5220–5230.
[10] B. G. McCarthy, R. M. Pearson, C.-H. Lim, S. M. Sartor, N. H. Damrauer, G. M. Miyake, *J. Am. Chem. Soc.* **2018**, *140*, 5088–5101.
[11] a) B. J. Coe, J. A. Harris, B. S. Brunschwig, J. Garin, J. Orduna, *J. Am. Chem. Soc.* **2005**, *127*, 3284–3285; b) M. Krompiec, I. Grudzka, M. Filapek, Ł. Skórka, S. Krompiec, M. Łapkowski, M. Kania, W. Danikiewicz, *Electrochim. Acta* **2011**, *56*, 8108–8114; c) G. J. Ryan, R. B. P. Elmes, S. J. Quinn, T. Gunnlaugsson, *Supramol. Chem.* **2012**, *24*, 175–188.
[12] a) R. Homer, T. Tomlinson, *Nature* **1959**, *184*, 2012–2013; b) P. S. Braterman, J. I. Song, *J. Org. Chem.* **1991**, *56*, 4678–4682.
[13] a) L. A. Summers, *The Bipyridinium Herbicides*, Academic Press, UK, **1980**; b) A. Pasi, *The Toxicology of Paraquat, Diquat and Morfamquat*, Huber, Bern, **1978**.
[14] a) J. Huang, Z. Yang, V. Murugesan, E. Walter, A. Hollas, B. Pan, R. S. Assary, I. A. Shkrob, X. Wei, Z. Zhang, *ACS Energy Lett.* **2018**, *3*, 2533–2538; b) Y.-T. Fanchiang, E. S. Gould, *Inorg. Chem.* **1978**, *17*, 1139–1141.
[15] Z. Mi, T. Zhou, W. Weng, J. Unruangsri, K. Hu, W. Yang, C. Wang, K. A. I. Zhang, J. Guo, *Angew. Chem. Int. Ed.* **2021**, *60*, 9642–9649; *Angew. Chem.* **2021**, *133*, 9728–9735.
[16] X. You, H. Ma, Y. Wang, G. Zhang, Q. Peng, L. Liu, S. Wang, D. Zhang, *Chem. Asian J.* **2017**, *12*, 1013–1019.
[17] M. S. Barclay, C. G. Elles, M. Caricato, *J. Phys. Chem. A* **2020**, *124*, 4678–4689.
[18] Y. Fujinami, J. Kuwabara, W. Lu, H. Hayashi, T. Kanbara, *ACS Macro Lett.* **2012**, *1*, 67–70.
[19] H. G. Roth, N. A. Romero, D. A. Nicewicz, *Synlett* **2016**, *27*, 714–723.
[20] a) P. Hohenberg, W. Kohn, *Phys. Rev.* **1964**, *136*, B864; b) W. Kohn, L. J. Sham, *Phys. Rev.* **1965**, *140*, A1133.
[21] E. Runge, E. K. U. Gross, *Phys. Rev. Lett.* **1984**, *52*, 997.
[22] a) J.-L. Brédas, D. Beljonne, V. Coropceanu, J. Cornil, *Chem. Rev.* **2004**, *104*, 4971–5004; b) M. Causá, J. D. Jonghe-Risse, M. Scarongella, J. C. Brauer, E. Buchaca-Domingo, J.-E. Moser, N. Stingelin, N. Banerji, *Nat. Commun.* **2016**, *7*, 12556.
[23] a) J. Preat, *J. Phys. Chem. C* **2010**, *114*, 16716–16720; b) B. Camino, M. D. L. Pierre, A. M. Ferrari, *J. Mol. Struct.* **2013**, *1046*, 116–123; c) S. Jungsuttiwong, R. Tarsang, T. Sudyoadsuk, V. Promarak, P. Khongpracha, S. Namuangruk, *Org. Electron.* **2013**, *14*, 711–722.
[24] a) G.-Z. Wang, R. Shang, W.-M. Cheng, Y. Fu, *Org. Lett.* **2015**, *17*, 4830–4833; b) M. Knorn, T. Rawner, R. Czerwieniec, O. Reiser, *ACS Catal.* **2015**, *5*, 5186–5193.
[25] Y. Luo, M. Wächtler, K. Barthelms, A. Winter, U. S. Schubert, B. Dietzek, *Chem. Commun.* **2018**, *54*, 2970–2973.
[26] Y. Tamura, S. Kwon, M. W. Chun, M. Ikeda, *J. Heterocycl. Chem.* **1978**, *15*, 425–427.
[27] Z. Wang, L. Wang, Q. Chen, M.-Y. He, *Synth. Commun.* **2018**, *48*, 76–84.
[28] J. S. Yadav, B. V. S. Reddy, B. B. M. Krishna, *Synthesis* **2008**, 3779–3782.
[29] H. Jiang, W. Yu, X. Tang, J. Li, W. Wu, *J. Org. Chem.* **2017**, *82*, 9312–9320.
[30] L. Wang, C. Wang, W. Liu, Q. Chen, M. He, *Tetrahedron Lett.* **2016**, *57*, 1771–1774.
[31] W. Fan, Q. Yang, F. Xu, P. Li, *J. Org. Chem.* **2014**, *79*, 10588–10592.
[32] P. Krishnan, V. G. Gurjar, *J. Appl. Electrochem.* **1995**, *25*, 792–796.
[33] a) S. R. Kandukuri, A. Bahamonde, I. Chatterjee, I. D. Jurberg, E. C. Escudero-Adán, P. Melchiorre, *Angew. Chem. Int. Ed.* **2015**, *54*, 1485–1489; *Angew. Chem.* **2015**, *127*, 1505–1509; b) E. L. Saux, M. Zanini, P. Melchiorre, *J. Am. Chem. Soc.* **2022**, *144*, 1113–1118; c) J. Zhang, Y. Li, R. Xu, Y. Chen, *Angew. Chem. Int. Ed.* **2017**, *56*, 12619–12623; *Angew. Chem.* **2017**, *129*, 12793–12797.
[34] L. Wylie, T. Blesch, R. Freeman, K. Hatakeyama-Sato, K. Oyaizu, M. Yoshizawa-Fujita, E. I. Izgorodina, *ACS Sustainable Chem. Eng.* **2020**, *8*, 17988–17996.
[35] W. Zhang, J.-T. Guo, Y. Yu, Z. Guan, Y.-H. He, *Tetrahedron* **2018**, *74*, 3038–3044.

Manuscript received: November 14, 2022
Accepted manuscript online: January 26, 2023
Version of record online: ■■, ■■